International Scientific Colloquium
Modelling for Electromagnetic Processing
Hannover, October 27-29, 2008

Particle transport in recirculated EM driven liquid metal flows

M. Kirpo, A. Jakovics, E. Baake, B. Nacke

Abstract

Coreless Induction Furnaces (CIF) are particularly suitable for experimental and numerical investigations of liquid metal flows due to simple geometry and relatively easy laboratory operation with model melts. Lagrangian particle tracing is performed together with Large Eddy Simulation (LES) of the turbulent flow in a laboratory CIF. It is shown, that preferential particle accumulation near the crucible side walls essentially depends on applied boundary conditions (BC), particle Stokes number and EM force. Separate particle tracks are also distinguished. The same numerical approach is successfully used for particle tracing in the industrial Induction Channel Furnaces (ICF).

Introduction

Electromagnetic heating and melting is very effective method for conducting material processing and production. The turbulent melt flow in induction furnaces and electromagnetic stirrers is formed by Lorentz forces and usually consists of one or several recirculated vortices. Depending on material properties different types of induction furnaces are suitable for production of high purity metal alloys, ceramics and glasses. The maximal intensities of the flow have characteristic values larger than 1 m/s in industrial equipment. Two types of induction furnaces are presented in this paper: CIF and ICF.

Flow in CIF (Fig. 1) consists in most cases of the two toroidal averaged flow vortices, which sizes and position depends on geometry and electromagnetic field distribution in the melt. Due to strong interaction between vortices, very rigorous melt stirring occurs [1] homogenizing melt temperature and species concentration. ICF are often used for copper or other non-ferrous alloy production and for steel casting. This type of furbaces is build like transformer with the iron core where the melt channel acts as a secondary coil. The iron core has large magnetic permeability and therefore reduces magnetic flux leakage increasing electrical efficiency, which can reach 90%. The channel is connected to the melt bath where characteristic flow velocities are 5-10 times smaller than in the channel.

It was established in experiments that measured temperature distribution in CIF is very homogeneous in the whole melt volume. This fact well corresponds to LES modeling results. Working temperatures in cast iron ICF are above 1500˚C and temperature homogenization and higher temperatures in the bath should be obtained for melt alloyage with additions, which can have higher melting temperature. Therefore calculation and optimization of the heat and mass transport is one of the tasks for computer simulation because alloyage species transport (for example carbon or silicon), homogenization or sedimentation can substantially influence quality of the final product in both furnace types or lifetime of the installation (ceramic channel erosion is another well-known problem of industrial ICF). Our experience shows that LES approach together with the Lagrangian particle tracing can be effectively used to analyze such problems. Computer modelling allows to study parameters of induction equipment before it is built and to improve energy efficiency of melting process. The aim of

this work is to study particle transport depending on different physical parameters using LES model and Lagrangian approach.

1. Cylindrical coreless induction furnace

Laboratory CIF (Fig. 1) was used in several series of experiments with Wood's metal [2] for analysis of the heat and mass transport processes. The Wood's melt flow in such induction furnace is formed by Lorentz forces and usually consists of several (two) recirculated vortices. Melt velocities (all components) in different points and for different inductor currents were measured with a permanent magnet probe [3]. Both experimental and transient numerical simulation results have introduced high-intensity ($\langle v' \rangle / v_{ch}$ >1,5) low-frequency velocity oscillations in the near-wall crucible regions, which are connected with exciting and decaying of large-scale turbulent vortices. These velocity pulsations are determinative for the heat and mass exchange in melt, especially in the zone between upper and lower eddies where the turbulent kinetic energy has explicit maximum (Fig. 2).

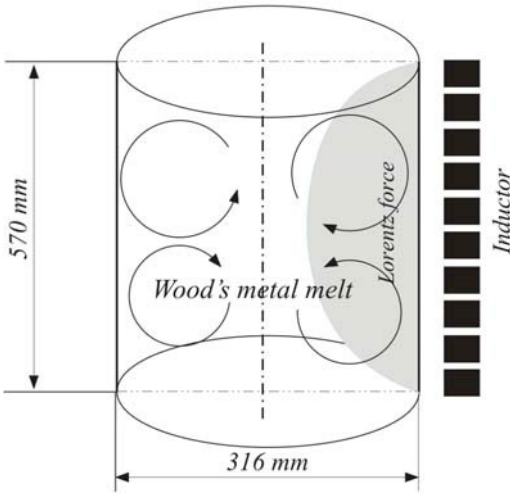

Figure 1. Design of laboratory CIF with sketch of typical vortices of the mean flow.

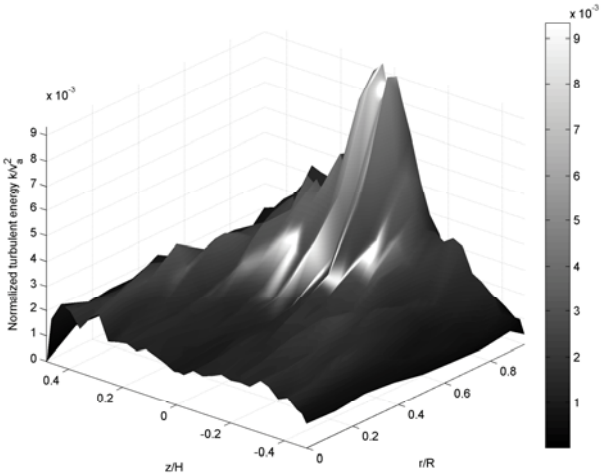

Figure 2. Experimental distribution of the normalized averaged axial pulsation kinetic energy k/v_A^2 (I = 2000 A, f = 395 Hz, B_0 = 0.098 T, $v_A = v_{Alfven}$ = 0.9 m/s).

The disperse particle motion in the conducting fluid under the influence of EM field is determined by several forces: Stokes drag, buoyancy force, EM force and lift force. The Stokes number can be introduced to describe the intensity of the particle interaction with the fluid. It is defined as the ratio of the particle fluid response time constant to an appropriate turbulence time scale (dissipation time) and also it can be estimated as $\mathrm{St} = \rho_p d_p^2 U /(18 \mu L)$ [4], where ρ_p is the particle density, d_p is the particle diameter, μ is the dynamic viscosity, U and L are characteristic velocity and distance.

For particle transport simulation the next force balance equation was solved in Lagrangian approach [5]:

$$\frac{d\vec{v}_p}{dt} = F_D(\vec{v} - \vec{v}_p) + \frac{\vec{g}(\rho_p - \rho)}{\rho_p} + \vec{F}_{pEM}, \qquad F_D = \frac{18\mu}{\rho_p d_p^2}\left(1 + 0.15\,\mathrm{Re}_p^{0.687}\right). \tag{1}$$

The particle Reynolds number Re_p and particle EM force [6] are given by

$$\mathrm{Re}_p = \frac{\rho d_p \left|\vec{v}_p - \vec{v}\right|}{\mu}, \qquad \vec{F}_{pEM} = -\frac{3}{2}\frac{\sigma - \sigma_p}{2\sigma + \sigma_p} V_P \vec{f}_{EM}, \tag{2}$$

where σ is the electrical conductivity, V_p is volume of the particle and $\vec{F}_{EM}$ is the specific magnetic Lorentz force. Particle EM force (2) is a key for EM separation process, which can be used to remove impurities from the melt or to accumulate certain particles near the working boundary of the final product if particle and melt electrical conductivities are different.

LES particle tracing was performed with several important assumptions: particle-particle interaction is negligible, all particles are solid rigid spheres and particles do not affect the structure and velocities of the flow. Two different kinds of particle injections were used. The first was to put several spherical particles of different densities and diameters, respectively with different Stokes numbers to the melt. This allows trailing unsteady particle trajectory and velocity at every time. The later is to distribute large amount of particles regularly on the planes inside the melt, therefore trailing distribution of the particle cloud at different time moments.

Surface injections of 30000 particles (d_p = 1 mm) were placed on two orthogonal meridian planes (x = 0 and y = 0 in Cartesian coordinates) in CIF (Fig. 1). All particles were injected at t = 0 (i.e. at the start of transient simulation) and about 60 seconds of the flow were computed. In most simulations the difference between the particle and fluid densities was 1.1 times (ρ_p = 8545, 9400, 10340 kg/m^3). The Stokes number for all 1 mm large particles is close to 0.08 with small variations depending on density.

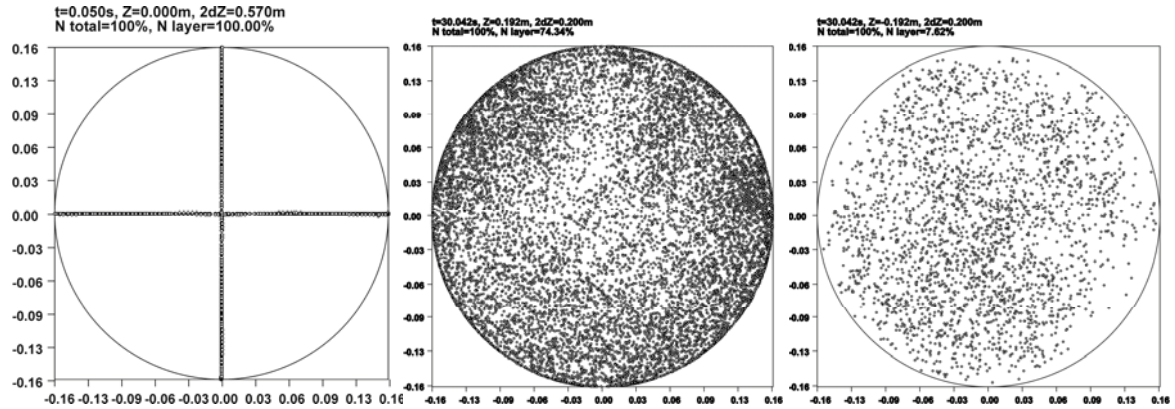

a) b) c)

Figure 3. Particle positions in the flow (ρ_p =0.9 ρ = 8545 kg/m^3, σ_p=σ, no-slip). View from the top: a) initial particle distribution at t=0; b) particles from 0.092 < z < 0.285 at t = 30 s; c) particles from -0.285 < z < -0.092 at t = 30 s.

The average flow velocity in the crucible is about 0.1 m/s. Introducing particle cloud on orthogonal planes (Fig. 3a) the mixing time, which corresponds to time when angular particle distribution becomes almost homogeneous, can be estimated as 10 s if particles are injected at once after the LES start from the converged k-ε or 5 s if the particles are injected into the fully developed turbulent flow. Lighter particles concentrate mainly in the top half of the melt (z > 0.092 m, ≈75% of all particles) occupying mainly near-wall region there while in the bottom their accumulation near the crucible wall is reduced (Fig. 3b and 3c). This difference near the crucible wall is determined by buoyancy and drag force directions: is it

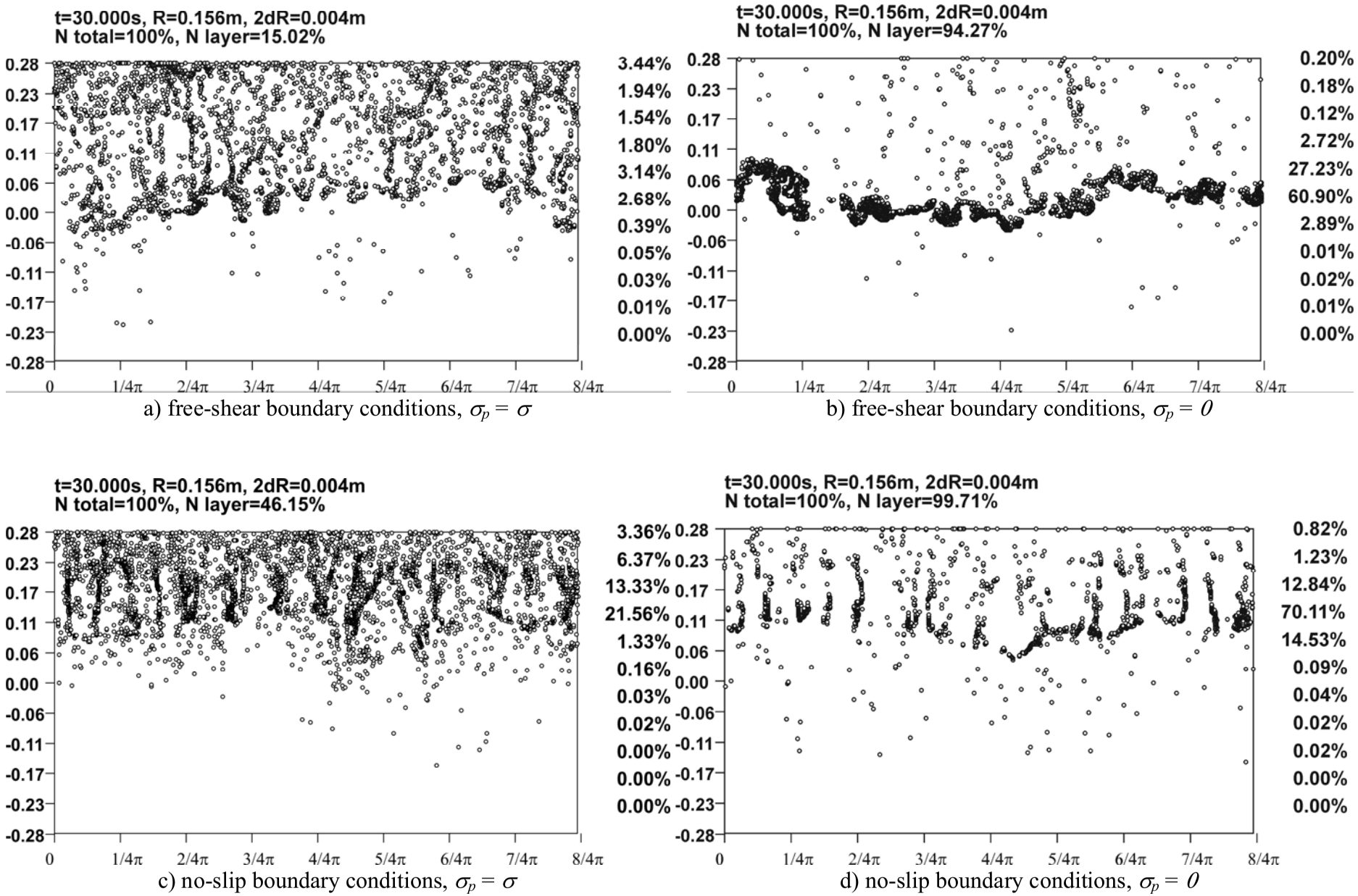

a) free-shear boundary conditions, $\sigma_p = \sigma$

b) free-shear boundary conditions, $\sigma_p = 0$

c) no-slip boundary conditions, $\sigma_p = \sigma$

d) no-slip boundary conditions, $\sigma_p = 0$

Figure 4. Angular particle distribution in 4 mm thick layer near the side crucible wall at t = 30 s, $\rho_p = 0.9\rho = 8545$ kg/m^3. View from the outside of the crucible. Particle injection is performed into k-ε calculated meridian flow at t = 0.

agrees or not. As a result particle motion near the crucible wall at top half of the crucible is braked ($v_p < v$), but at the bottom half it is promoted ($v_p > v$) and particles faster pass this near-wall region. An exactly opposite phenomenon develops near the symmetry axis. Particle distribution near the symmetry axis r=0 is approximately the same for the both top and bottom half of the melt.

Below results will represent only the particle clouds with $\rho_p = 0.9\rho = 8545$ kg/m^3 due to common particle accumulation tendencies [7] for $\rho_p = 1.1\rho$ (heavier particles will mainly accumulate in the bottom half of the melt – in the bottom vortex). Particle concentration distribution becomes almost time independent at t = 30 s. Lighter particles are mainly concentrated in the top half of the 4 mm near-wall layer. Free-slip BC increase near wall flow velocities and release angular velocity oscillations. As a result particle distribution in the near wall region of the upper vortex is relatively homogeneous, however, higher particle accumulation can be noticed near the top surface and between the "main" eddies if $\sigma_p = \sigma$ (Fig. 4a). If no-slip BC are applied, then particle concentration in this near-wall layer increases 3 times (Fig. 4c) and maximum of particle accumulation moves up to the upper vortex middle region and "periodic" vertical stripes of particles are noticed here. Such particle distribution in stripes is determined by the reduced axial and angular velocities due to near-wall shear.

If the previously described conducting particles with $\sigma_p = \sigma$ are replaced by non-conducting particles with $\sigma_p = 0$, then due to EM force action at least 95% of all particles are concentrated in this near-wall layer. The most of these particles are accumulated in the zone between vortices (Fig. 4b) where $\vec{v}_{average} = 0$ if free-shear BC are applied to the side wall. However, no-slip BC again introduce explicit vertical cluster-like particle stripes with maximal particle accumulation on the half height of the upper vortex (Fig. 4d), which are defined by small mixing intensity in angular direction and smaller characteristic axial velocities near the wall. In this case almost all particles are concentrated in the mentioned 4 mm near-wall layer.

2. Induction channel furnaces

Lagrangian particle tracking was performed on a model of industrial 300 kW induction channel furnace for cast iron (Fig. 5). The flow velocities can reach 2 m/s in the ICF channel and the flow is highly turbulent. The flow structure in the channel is determined by the Lorentz force distribution: Lorentz forces are directed to the center of the channel with the maximal force density near the inner channel furnace. Therefore, flow can form single loop (Fig. 5a) or double loop (Fig. 5b) vortices in the channel cross-sections where rotation axis is directed along the channel at different time moments. Flow structure substantially changes in the channel exit to the neck, where eddy rotation axis becomes orthogonal to the previous direction and flow intensity decreases.

Several 0.2 mm particles with $\rho_p = 5250$ kg/m^3 are released in the different ICF parts, five of them - near the bottom central point in the channel. Their trajectories (Fig. 5c) show presence of the mainly thermally determined transit melt flow in the channel, which intensity is much smaller than the intensity of the turbulent vortices in the channel cross-sections. The direction of the channel transit flow depends on the shift of temperature maximum location in the channel. Particles tracks represent the previously mentioned properties of vortices near the channel exits. Particles tracing allows to estimate this transit flow velocity, which in this case is near 7 cm/s, while the average particle velocity is above 50 cm/s.

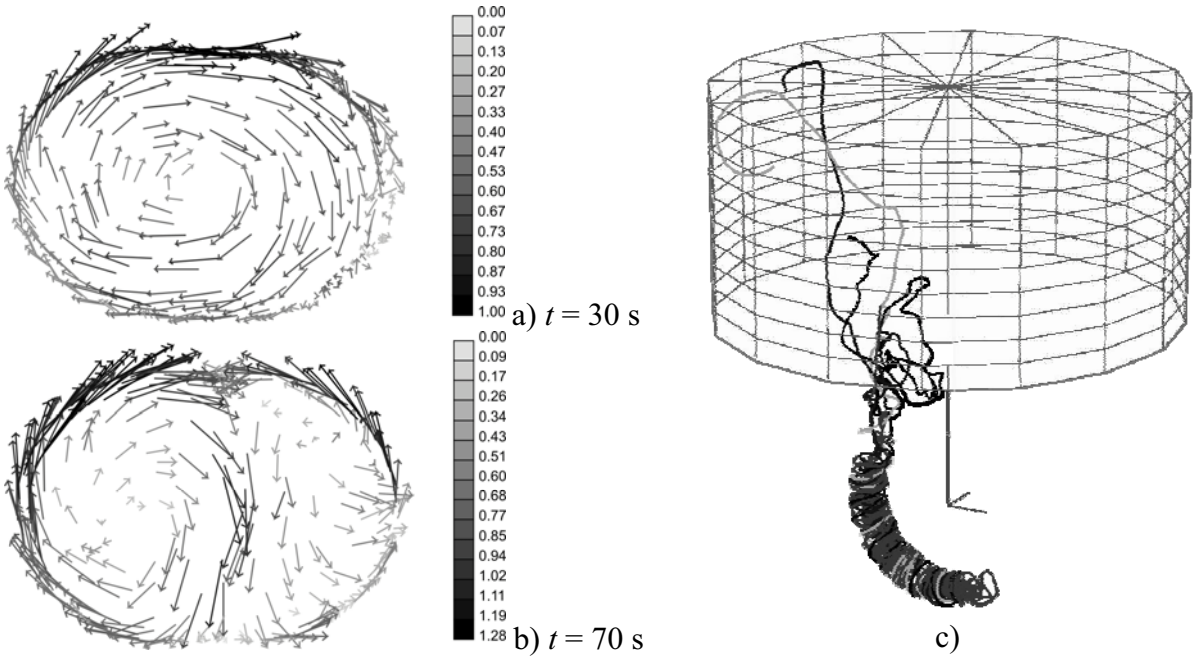

Figure 5. LES calculated instantaneous velocities in the channel cross-section of 300 kW ICF and 50 s tracks of 0.2 mm particles ($\sigma_p = 0$, $\rho_p \approx 0.75\rho = 5250$ kg/m^3).

Conclusions

CIF Lagrangian particle tracing has shown preferential accumulation of large particles in the near-wall crucible region. Particles concentrate there in the top ($\rho_p/\rho < 1$), middle ($\rho_p/\rho = 1$) or bottom ($\rho_p/\rho > 1$) half depending on density ratio ρ_p/ρ. No-slip boundary conditions and EM field can lead to collection of almost all 1 mm particles in the near-wall crucible region. Boundary conditions influence angular homogenization of the particle volume fraction and EM field can completely break the non-conducting particle motion. Particle transport modeling shows very intensive vortical flow in the channel cross-sections and transit flow existence in ICF, which averaged intensity can be estimated with the proposed method.

References

[1] E. Taberlet, Y. Fautrelle. *Turbulent stirring in an experimental induction furnace*, J. Fluid Mech., vol. 159, 1985, pp. 409–431.
[2] A. Eggers. *Untersuchungen der Schmelzenströmung und des Wärmetransports im Induktions-Rinnenofen,* PhD thesis, VDI, Düsseldorf, 1993
[3] R. Ricou, C. Vives. *Local velocity and mass transfer measurements in molten metals using an incorporated magnet probe*, Int. J. Heat and Mass Transfer, vol. 25, 1982, pp. 1579–1588
[4] C. T. Crowe. *Multiphase flow handbook*. New York: CRC Press 2006
[5] R .Clift, J. R. Grace, M. E. Weber. *Bubbles, Drops and Particles*. New York: Academic Press, 1978
[6] D. Leenov, A. Kolin. *Theory of Electromagnetophoresis. I.Magnetohydrodynamic Forces Experienced by Spherical & Symmetrically Oriented Cylindrical Particles*. J. Of Chemical Phys., vol. 22(4), 1954, pp. 683–688
[7] M. Kirpo, A. Jakovičs, B. Nacke, E. Baake. *Particle transport in recirculated liquid metal flows*. Compel, vol. 27(2), 2008, pp. 377–386

Authors

Kirpo, Maksims
Dr.-Phys. Jakovics, Andris
University of Latvia
Faculty of Physics and Mathematics
Zellu str. 8
LV-1002 Riga, Latvia
e-mail: maksims.kirpo@lu.lv

Prof. Dr.-Ing. Baacke, Egbert
Prof. Dr.-Ing. Nacke, Bernard
Leibniz University of Hannover
Institute of Electrotechnology
Wilhelm-Busch-Str. 4
30167 Hannover
e-mail: baake@ewh.uni-hannover.de